IVYSPRING INTERNATIONAL PUBLISHER

Theranostics

2016; 6(1): 1-13. doi: 10.7150/thno.12167

Research Paper

ICAM-1-Targeted, Lcn2 siRNA-Encapsulating Liposomes are Potent Anti-angiogenic Agents for Triple Negative Breast Cancer

Peng Guo[1,2,3†], Jiang Yang[2,3†], Di Jia[2,3], Marsha A. Moses[2,3‡] and Debra T. Auguste[1,2,3‡✉]

1. Department of Biomedical Engineering, The City College of New York, 160 Convent Avenue, New York, NY 10031, United States
2. Vascular Biology Program, Boston Children's Hospital, 300 Longwood Avenue, Boston, MA 02115, United States
3. Department of Surgery, Harvard Medical School and Boston Children's Hospital, 300 Longwood Avenue, Boston, MA 02115, United States

†These authors contributed equally to this work, and are co-first authors.

‡These authors contributed equally to this work, and are co-last authors.

✉ Corresponding author: Email: dauguste@ccny.cuny.edu

Received: 2015.03.18; Accepted: 2015.09.16; Published: 2016.01.01

Abstract

Lipocalin 2 (Lcn2) is a promising therapeutic target as well as a potential diagnostic biomarker for breast cancer. It has been previously shown to promote breast cancer progression by inducing the epithelial to mesenchymal transition in breast cancer cells as well as by enhancing angiogenesis. Lcn2 levels in urine and tissue samples of breast cancer patients has also been correlated with breast cancer status and poor patient prognosis. In this study, we have engineered a novel liposomal small interfering RNA (siRNA) delivery system to target triple negative breast cancer (TNBC) via a recently identified molecular target, intercellular adhesion molecule-1 (ICAM-1). This ICAM-1-targeted, Lcn2 siRNA- encapsulating liposome (ICAM-Lcn2-LP) binds human TNBC MDA-MB-231cells significantly stronger than non-neoplastic MCF-10A cells. Efficient Lcn2 knockdown by ICAM-Lcn2-LPs led to a significant reduction in the production of vascular endothelial growth factor (VEGF) from MDA-MB-231 cells, which, in turn, led to reduced angiogenesis both in vitro and in vivo. Angiogenesis (neovascularization) is a requirement for solid tumor growth and progression, and its inhibition is an important therapeutic strategy for human cancers. Our results indicate that a tumor-specific strategy such as the TNBC-targeted, anti-angiogenic therapeutic approach developed here, may be clinically useful in inhibiting TNBC progression.

Key words: ICAM-1, Lipocalin-2, liposomal siRNA, triple-negative breast cancer, angiogenesis

Introduction

Small interfering RNAs have been recognized as a new class of gene-silencing therapeutics for the treatment of a variety of diseases including cancer,(1–3) yet the clinical use of an siRNA as a cancer therapeutic is limited by its inefficient delivery to the target cell population. The short half-life ($t_{1/2}$ – 1.5 min) of siRNA in the bloodstream and poor cytoplasmic delivery have challenged its translation to the clinic.(4) In recent years, liposomal siRNA delivery systems have been developed that augment siRNA tumor specificity and accumulation.(5–8) An ideal siRNA delivery system for the treatment of cancer should selectively target cancer cells, deliver siRNA to the cytoplasm, and silence the target protein to hinder tumor growth and progression.

TNBC is defined by the absence of the estrogen receptor (ER), the progesterone receptor (PR), and the human epidermal growth factor receptor type 2

(HER-2).(9) TNBCs represent 15–20% of all breast cancers, occurring more frequently in women under 50 years of age, African American women, and individuals carrying mutations in the breast cancer early onset 1 (BRCA1) gene.(9) The significant growth and metastasis of TNBC tumors, coupled with fewer treatment options, have resulted in higher mortality rates for TNBC relative to HER2 and ER positive breast cancers.(10–12) We have previously demonstrated that ICAM-1 is highly overexpressed in human TNBC tissues and cell lines.(13) We further showed that ICAM-1 antibody-functionalized iron oxide nanoparticles facilitated efficient *in vivo* TNBC tumor targeting, representing a promising opportunity to develop a TNBC-targeted nanomedicine.(13)

A widely accepted, therapeutic strategy for the treatment of cancer is to control angiogenesis, the formation of new blood vessels from pre-existing ones, a process which is a hallmark of solid tumor growth and progression.(14–16) During angiogenesis, regulated by a dynamic array of factors, endothelial cells proliferate, migrate and infiltrate the tumor. Anti-angiogenic therapies are attractive as they reduce tumor growth by limiting the tumor's nutrient and oxygen supply via targeting the vasculature. Lcn2 (also known as neutrophil gelatinase-associated lipocalin (NGAL)), a 25-kDa protein and a member of the lipocalin protein superfamily, is a regulator of angiogenesis.(17,18) Increased Lcn2 levels have been reported in a variety of human epithelial cancers, including breast cancer (increased expression of Lcn2 in TNBC shown in **Figure S1**).(19) Elevated levels of Lcn2 have been detected in the urine of breast cancer patients and correlate with progression of breast cancer, suggesting Lcn2 is a non-invasive urinary diagnostic and prognostic marker for breast cancer.(17,20) We have previously shown that Lcn2 may actively promote breast cancer progression via inducing the epithelial to mesenchymal transition in breast cancer cells (20) as well as by stimulating neovascularization. We have demonstrated that Lcn2 secreted from TNBC cells stimulates neovascularization through increasing the level of vascular endothelial growth factor (VEGF) and that transient knockdown of Lcn2 in breast cancer cells resulted in reduced tumor angiogenesis, making it an ideal TNBC anti-angiogenic target.(18)

In the present study, we engineered a novel TNBC-targeted, anti-angiogenic approach to suppress tumor vessel formation. We have previously shown that ICAM-1 is upregulated in TNBC cells and can serve as a molecular target for TNBC.(13) Here, we demonstrate that liposomes combining ICAM-1 targeting with Lcn2 siRNA delivery (ICAM-Lcn2-LP) significantly inhibit TNBC angiogenesis *in vitro* and *in vivo* and may represent a potential therapeutic approach for the treatment of TNBC.

Materials and Methods

Materials

1,2-dioleoyl-sn-glycero-3-phosphocholine (DOPC), 1,2-dioleoyl-3-dimethylammonium-propane (DODAP), and 1,2-distearoyl-sn-glycero-3-phosphoethanolamine-N-[carboxy(polyethylene glycol)-2000] (DSPE-PEG-COOH) were purchased from Avanti Polar Lipids (Alabaster, AL, USA). Dulbecco's phosphate buffered saline (PBS), Quant-iT ™ RNA Assay Kit, 0.25% trypsin/2.6 mM ethylenediaminetetraacetic acid (EDTA) solution, uPAGE 4-12% Bis-Tris gels, Gibco® Dulbecco's Modified Eagle Medium (DMEM), and Gibco®DMEM/F12(1:1) were purchased from Invitrogen (Carlsbad, CA, USA). EGM-2 BulletKits and EGM-2MV BulletKit media were purchased from Lonza (Allendale, NJ, USA). Quantum Simply Cellular microbeads were purchased from Bangs Laboratory (Fishers, IN, USA). Mouse anti-human ICAM1 monoclonal antibody (aICAM1), mouse anti-human Lcn2 antibody, immunoglobulin G (IgG) isotype control, NorthernLight® 557 (NL557)-conjugated donkey anti-mouse IgG, and VEGF ELISA kit were purchased from R&D Systems (Minneapolis, MN, USA). RNeasy Mini Kit was purchased from QIAGEN (Valencia, CA, USA). Phycoerythrin (PE)-conjugated mouse anti-human ICAM1 antibody (PE-aICAM1) and PE-conjugated mouse IgG isotype (PE-IgG) were purchased from BioLegend (San Diego, CA, USA). 1-Ethyl-3-(3-dimethylaminopropyl) carbodiimide hydrochloride (EDC), N-hydroxysuccinimide (NHS), bovine serum albumin (BSA), and anhydrous dimethyl sulfoxide (DMSO) were purchased from Sigma-Aldrich (St. Louis, MO, USA). FLOAT-A-LYZER G2 dialysis tubing (MWCO 300 kDa) was obtained from Spectrum Laboratories (Rancho Dominguez, CA, USA). Slide-A-Lyzer dialysis cassette (MWCO 20 kDa) was obtained from Pierce Biotechnology (Rockford, IL, USA). Matrigel (growth factor-reduced) was purchased from BD (Franklin Lakes, NJ, USA). Lab-Tek II Chamber Slide System was obtained from Thermo Fisher Scientific (Pittsburgh, PA, USA). Fluorogel with tris buffer was purchased from Electron Microscopy Sciences (Hatfield, PA, USA). Dojindo cell counting kit was purchased from Dojindo Molecular Technologies (Rockville, MD). Diff-Quik Stain Set was purchased from Siemens Healthcare Diagnostics (Tarrytown, NY, USA). Anti-glyceraldehyde-3-phosphate dehydrogenase (GAPDH) antibody was purchased from Millipore (Billerica, MA, USA). RIPA Lysis buffer was purchased from Santa Cruz Biotechnology (Dallas, TX, USA). Western Lightning Plus-ECL Enhanced Chemiluminescence Substrate

was purchased from PerkinElmer (Waltham, MA, USA).

Cell Culture

Human TNBC MDA-MB-231 cells and non-neoplastic human MCF10A cells were obtained from American Type Culture Collection (ATCC, Manassas, VA, USA). Human microvascular endothelial cells (HMVEC) and human umbilical vein endothelial cells (HUVEC) were purchased from Lonza (Allendale, NJ, USA). MDA-MB-231, MCF10A, HUVEC and HMVEC were cultured in DMEM, DMEM/F12(1:1), EGM-2 BulletKit and EGM-2MV BulletKit media with recommended supplements, respectively. All cells were cultured in a 37°C humidified incubator with 5% CO_2.

Preparation of Immunoliposomes

The ICAM-1 antibody labeled, Lcn2 siRNA encapsulating, pH-responsive liposomes (ICAM-Lcn2-LPs) were prepared as described previously.(21,22) A lipid formulation consisting of DOPC:DODAP:DSPE-PEG-COOH (85:10:5 molar ratio) was used to prepare liposomes. 50 μmol lipid mixture was solubilized in chloroform and dried under a dry nitrogen stream. The resulting lipid film was dissolved in 1 mL DMSO:EtOH (7:3, v:v). The lipid solution was injected in 9 mL of 15 μg/mL Lcn2 siRNA or scrambled siRNA in phosphate buffered saline (PBS, pH 7.4) while being rigorously agitated to yield a 5 mM lipid solution. After 10 freeze-thaw cycles, lipid solution was extruded via a NorthernLipids Extruder with a 100 nm polycarbonate nanoporous membrane. After extrusion, the liposome solution was dialyzed in PBS (pH 7.4) using a Slide-A-Lyzer dialysis cassette (MWCO 20 kDa) overnight at room temperature (RT).

Liposomes were conjugated to ICAM-1 antibody via the DSPE-PEG-COOH anchor. EDC (2 mg) and NHS (3 mg) were mixed with 1 mmol of lipid (liposomes) in PBS (pH 7.4) and incubated for 6 h at RT. A Slide-A-Lyzer dialysis cassette (MWCO 10 kDa) was used to remove unreacted EDC and NHS. Next, aICAM1 or the IgG isotype was added to EDC-modified liposomes at a molar ratio of 1:1000 (antibody:phospholipid) and incubated overnight at RT. Unreacted antibodies were removed by using a FLOAT-A-LYZER G2 dialysis tubing (MWCO 300 kDa). In liposome binding experiments, ICAM-1 antibody-labeled, rhodamine-dextran encapsulating liposomes (ICAM-RD-LPs) were prepared and tested. For ICAM-RD-LPs, the preparation process was similar as ICAM-Lcn2-LPs with the exception being that the 1 mL lipid solution was added to a 9 mL rhodamine-dextran solution (1 mg/mL).

The density of antibodies conjugated on liposomes was quantified. Liposomes cannot be detected by flow cytometry because of their size, therefore, 2 μm borosilicate beads were encapsulated within DOPC:DODAP:DSPE-PEG-COOH (85:10:5, mol:mol:mol) liposomes by sonicating small unilamellar liposomes with microbeads in PBS for 6 h. Microbeads were rinsed three times in PBS via suspension-spin cycles to separate free liposomes. Conjugation of PE-ICAM-1 antibody or PE-IgG (nonspecific binding) to microbead encapsulating liposomes was performed using EDC/NHS chemistry. The surface density of ICAM-1 antibody conjugated to each microbead was determined with reference to Quantum Simply Cellular microbeads, which have defined numbers of antibody binding sites per bead. Liposome size and zeta potential were measured by dynamic light scattering on a Zeta-PALS analyzer (Brookhaven Instruments, Holtsville, NY) in PBS (pH 7.4).

Lcn2 siRNA Encapsulation Efficiency

A Quant-It RiboGreen RNA assay was performed to determine the encapsulation efficiency of siRNA within the liposome samples according to the manufacturer's protocol. siGENOME SMARTpool human Lcn2 siRNA constructs and siGENOME Non-Targeting siRNA Pool were purchased from Dharmacon (Lafayette, CO). Lcn2 siGENOME SMARTpool siRNA is composed of four Lcn2 siRNAs: D-003679-05, UGGGCAACAUUAAGAGUUA; D-003679-03, GAAGACAAGAGCUACAAUG; D-003679-02, GGAGCUGACUUCGGAACUA; D-003679-01, GAGCUGACUUCGGAACUAA. A siRNA concentration calibration curve was generated from serially diluted siRNA standard solutions and appropriate backgrounds measured on a SpectraMaxPlus 384 UV-Visible Spectrophotometer (excitation 500 nm, emission 525 nm). Next, the 20 μL liposome sample was added to 1 mL of 0.5% Triton X-100 in a microcentrifuge tube and vortexed for 1 min. The microcentrifuge tube was incubated in 37 °C incubator for 1 h. Triton X-100 is a surfactant that lyses liposomes. The 200 μL of siRNA containing Triton X-100 solution was homogeneously mixed with 200 μL 200-fold diluted Quant-It RiboGreen RNA reagent working solution for 5 min. The resulting solution was added to at least three wells per each sample of a flat bottom 96-well cell culture plate, and measured for fluorescence. The 0.5% Triton X-100 solution mixed with 200-fold diluted Quant-It RiboGreen RNA reagent working solution was used as a blank control. The encapsulation efficiency (%) is the encapsulated siRNA concentration divided by the initial siRNA concentration multiplied by 100.

Immunoliposome Binding

Quantitative analysis of liposome binding to MDA-MB-231 (TNBC) and MCF10A (control) cells was studied by flow cytometry as previously described.(21,22) 10^6 cells were placed in each well of a 6-well cell culture plate and incubated for 4 h at 37°C with (1) rhodamine-dextran encapsulated nonspecific (IgG) liposomes (IgG-RD-LPs) and (2) ICAM-RD-LPs. The concentration used was 1 μmol lipid/10^6 cells. All liposome-treated cells were washed with PBS, harvested using a 0.25% trypsin/2.6 mM EDTA solution, and washed with PBS (pH 7.4) three times. Binding data were acquired using a BD FACSCalibur flow cytometer and analyzed using FlowJo software. The specific cell uptake of ICAM-RD-LPs with reference to non-specific IgG-RD-LPs was calculated by dividing the mean fluorescence intensity of ICAM-RD-LP stained cells by that of the IgG-RD-LP stained cells.

Lcn2 siRNA Knockdown Efficiency

RT-PCR was used to examine Lcn2 mRNA expression in MDA-MB-231 cells following liposome treatment. 3×10^5 MDA-MB-231 cells were seeded in 6-well plates and incubated for 24 h. Cells were treated with (1) PBS (control), (2) Free Lcn2 siRNA, (3) ICAM-SCR-LP, (4) Lcn2-LIPO, (5) IgG-Lcn2-LP, and (6) ICAM-Lcn2-LP for 6 h at the final siRNA concentration of 100 nM. Cells were rinsed three times with PBS and further grown for 72 h. RNA was isolated using the RNeasy Mini Kit (QIAGEN) according to the manufacturer's protocol. cDNA was synthesized using the Superscript Vilo Kit (Life Technologies) , and levels of Lcn2 were quantified using StepOnePlus Real-Time PCR System (Applied Biosystems, Carlsbad, CA, USA). All PCR samples were referenced to the expression of Glyceraldehyde 3-phosphate dehydrogenase (GAPDH).

Immunoblot Analyses

MDA-MB-231 cell lysates were collected using RIPA Lysis Buffer (Santa Cruz Biotechnology). Proteins were separated on NuPAGE 4-12% Bis-Tris gels (Invitrogen) and transferred to a nitrocellulose membrane (Bio-Rad). The membrane was blocked in TBST (Tris Buffered Saline with 0.2% Tween-20) with 5% milk and incubated with the anti-human Lcn2 antibody (R&D Systems,1:1000 dilution) or anti-glyceraldehyde-3-phosphate dehydrogenase (GAPDH) antibody (Millipore, 1:10,000 dilution) in TBST with 2% milk overnight at 4°C, followed by incubation with corresponding secondary antibodies (Pierce) for 1 hour at room temperature as previously reported by us.(18,20,23) The membranes were developed using Western Lightning Plus-ECL Enhanced Chemiluminescence Substrate (PerkinElmer). Lcn2 protein levels were quantified via densitometric analysis using NIH ImageJ software.

Measurement of Human VEGF Protein Levels in Conditioned Media (CM)

To harvest CM, MDA-MB-231 cells were first treated (1) PBS (control), (2) Free Lcn2 siRNA, (3) ICAM-SCR-LP, (4) Lcn2-LIPO, (5) IgG-Lcn2-LP, and (6) ICAM-Lcn2-LP at the final siRNA concentration of 100 nM as described above, and grown for 72 h as described in the Lcn2 siRNA knockdown study. Cells were then rinsed twice with PBS, and cultured in 1 mL of serum-free DMEM for another 24h. After 24h, CM was collected and centrifuged at 1,200 rpm for 5 min to remove suspended cells. Supernatant were collected and re-centrifuged at 10,000 rpm for 5 min to remove cell debris and organelles. The final supernatant was collected for further *in vitro* anti-angiogenesis studies as we previously reported.(18,20) In the endothelial proliferation studies, we used 1 mL Endothelial Basal Medium to replace DMEM in CM production because HUVEC and HMVEC cells grow poorly in DMEM without serum. A commercially available human VEGF ELISA kit from R&D Systems (Minneapolis, MN, USA) was used to quantify the levels of VEGF in CM obtained from MDA-MB-231 cells treated with different samples, according to manufacturer's instructions.

Endothelial Cell Proliferation

Endothelial cell proliferation was measured using our previously reported protocol with modifications.(23,24) 5×10^3 human endothelial cells (HMVECs or HUVECs) were plated in each well of a 96-well plate and treated for 48 h with CM harvested from MDA-MB-231 treated with (1) PBS (control), (2) Free Lcn2 siRNA, (3) ICAM-SCR-LP, (4) Lcn2-LIPO, (5) IgG-Lcn2-LP, and (6) ICAM-Lcn2-LP at the final siRNA concentration of 100 nM as described above. The human endothelial cell proliferation was analyzed using a Dojindo cell counting kit using the protocol from the Dojindo Molecular Technologies (Rockville, MD, USA).

Endothelial Cell Migration

Human endothelial cells (HUVEC or HMVEC, 10^5 cell per well) were seeded onto COSTAR transwell inserts with permeable support polycarbonate membrane and an 8 μm pore size in a 24-well plate as previously reported by us.(18,20,25) DMEM without fetal bovine serum and CM harvested from MDA-MB-231 treated with (1) PBS, (2) Free Lcn2 siRNA, (3) ICAM-SCR-LP, (4) Lcn2-LIPO, (5) IgG-Lcn2-LP, and (6) ICAM-Lcn2-LP at the final siRNA concentration of 100 nM as described above were added to the upper and lower wells, respectively. The cells were incu-

bated and allowed to migrate for 20 h. The cells on the reverse side of transwell membrane facing the lower chamber after transmigrating through the 8-μm pores of tranwell membrane were stained with Diff-Quik Stain Set. Four fields were counted for each sample.

Endothelial Tube Formation

We performed endothelial tube formation experiment using a previously reported protocol with modifications.(26) A 48-well plate was coated with 125 μL Matrigel (growth factor-reduced, 8–10 μg/μL, BD) and allowed to solidify at 37 °C for 1 h. HMVEC or HUVEC cells (1×10^5) were resuspended in 200 μL CM harvested from MDA-MB-231 treated with (1) PBS (control), (2) Free Lcn2 siRNA, (3) ICAM-SCR-LP, (4) Lcn2-LIPO, (5) IgG-Lcn2-LP, and (6) ICAM-Lcn2-LP at the final siRNA concentration of 100 nM as described above, and were then layered onto the Matrigel and the formation of tube-like structures after 20 h was determined. The number of branches in the tube-like structures was quantified and compared between different samples.

Chicken Chorioallantoic Membrane (CAM) Assay

The CAM assay was performed as previously reported by us.(24–28) Fertilized chicken embryos (Charles River Laboratories, North Franklin, CT) were cultured *in-ova*. At developmental day 7, 5 μL of serum-free media (1) (negative control) or CMs harvested from MDA-MB-231 cells treated with the following agents: (2) PBS (sham), (3) IgG-Lcn2-LP, and (4) ICAM-Lcn2-LP at the final siRNA concentration of 100 nM as described above, was applied to a piece of filter paper-based substrate (2 mm in diameter) on the CAM. At 48 h, CAM images were recorded using a Nikon SMZ1500 microscope. The angiogenic response surrounding the substrate was scored from 0-4 as reported previously.(29) CAMs without newly formed vessels surrounding the substrate were scored as 0 (no angiogenic response). CAMs with the most intense vessel formation in a spoke-wheel pattern were scored as 4 (strongest angiogenic response). CAMs with samples that recruited fewer and smaller vessels were scored as 1-3, depending on the intensity as described previously.(29) A sum of 41 eggs was scored with at least 9 eggs tested for each sample. Statistical significance was achieved by *p*-value equal or smaller than 0.05.

Statistical Analysis

All of experimental data was obtained in triplicate unless otherwise indicated and are presented as mean ± standard deviation. Statistical comparison by analysis of variance was performed at a significance level of $p < 0.05$ based on a Student's *t*-test.

Results

Characterization of Immunoliposomes

The gene and protein levels of ICAM-1 are highly increased in human TNBC tissues and cells with significantly lower expression in human normal mammary tissues and epithelial cells (as shown in **Figures S2-4**). We have previously reported that the ICAM-1 antibody is an efficient TNBC-targeting ligand *in vivo*.(13) By conjugating ICAM-1 antibodies to liposomes, encapsulated siRNA can be delivered specifically to TNBC tumors and cells. We engineered ICAM-Lcn2-LPs to inhibit the angiogenic activities in TNBC (scheme illustrated in **Figure 1**). The pH-responsive, liposomal delivery vehicle is composed of a mixture of DOPC, DODAP, and DSPE-PEG-COOH. DODAP was incorporated in the liposome to respond to the acidic endosomal environment by increasing its cationic character, fusing with the endosomal membrane, and delivering the encapsulated siRNA to the cytoplasm.(30,31) The PEG chain (2 kDa) in DSPE-PEG-COOH has been shown to improve the liposome biocompatibility and circulation period.(32,33) The carboxyl group of DSPE-PEG-COOH functions as a site for either the ICAM-1 antibody or the nonspecific immunoglobulin G (IgG) conjugation. EDC/NHS chemistry was used to covalently bond the carboxylic acid on DSPE-PEG-COOH to a primary amine group presented on the ICAM-1 antibody or the IgG.

Three liposome formulations were tested for efficacy of siRNA delivery: (1) ICAM-Lcn2-LP, (2) Nonspecific IgG-conjugated, Lcn2 siRNA-encapsulating liposomes (IgG-Lcn2-LP), and (3) Lcn2 siRNA-Lipofectamine complexes (Lcn2-LIPO). Lipofectamine is a commercial siRNA transfection reagent used here as a positive control. Formulated immunoliposomes were first characterized by dynamic light scattering to measure their hydrodynamic sizes and zeta-potentials (**Table 1**).

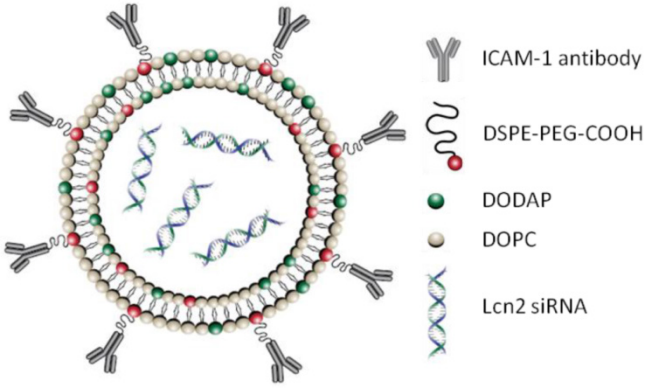

Figure 1. Schematic illustration of the designed ICAM-1 antibody-conjugated, Lcn2 siRNA-encapsulating liposome (ICAM-Lcn2-LP).

Table 1. Diameter, size distribution, zeta potential, siRNA loading, and antibody density of as-synthesized immunoliposomes.

Sample	Size (nm)	PDI	Zeta potential (mV)	Encapsulation Ratio (%)	Antibody density (molecules/μm²)	Antibody density (molecules/liposome)
ICAM-Lcn2-LP	114 ± 51	0.160	-14.8 ± 0.3	46.2 ± 2.6	3,497 ± 6	142.8 ± 0.2
IgG-Lcn2-LP	111 ± 60	0.220	-12.2 ± 2.6	42.0 ± 4.0	3,629 ± 132	140.5 ± 5.1
Lcn2-LIPO	703 ± 345	0.273	−3.4 ± 2.5	70.0 ± 2.0	N/A	N/A
ICAM-SCR-LP	118 ± 58	0.186	−11.4 ± 7.1	44.5 ± 6.6	3,497 ± 6	153.0 ± 0.3
ICAM-RD-LP	119 ± 60	0.185	−13.5 ± 9.9	47.1 ± 3.9	3,497 ± 6	155.6 ± 0.3
IgG-RD-LP	123 ± 67	0.193	−8.0 ± 3.0	46.7 ± 8.1	3,629 ± 132	172.5 ± 6.3

The hydrodynamic sizes of ICAM-Lcn2-LP, IgG-Lcn2-LP, and Lcn2-LIPO are 114 ± 51, 111 ± 60, and 703 ± 345 nm, respectively. Commercial Lcn2-LIPO complexes demonstrate a larger size than ICAM-Lcn2-LP and IgG-Lcn2-LP due to differences in preparation (electrostatic vs. extrusion). Liposomes smaller than 200 nm can evade capture by macrophages in the bloodstream and are thus more likely to circulate for longer times.(34,35) The zeta potentials for each vehicle are as follows: -14.8 ± 0.3 mV for ICAM-Lcn2-LP, -12.2 ± 2.6 mV for IgG-Lcn2-LP, and −3.4 ± 2.5 mV for Lcn2-LIPO. The siRNA encapsulation efficiencies of as-synthesized immunoliposomes are 46.2 ± 2.6% (ICAM-Lcn2-LP) and 42.0 ± 4.0% (IgG-Lcn2-LP), much lower than that of Lcn2-LIPO (70.0 ± 2.0%). The lower siRNA encapsulating efficiencies for ICAM-Lcn2-LP and IgG-Lcn2-LP may be due to repetitive extrusion and dialysis during liposome preparation whereas the electrostatic complex between Lipofectamine and siRNA retains a higher amount of siRNA. The antibody surface densities of the immunoliposomes are 142.8 ± 0.2 (ICAM-Lcn2-LP) and 140.5 ± 5.1 (IgG-Lcn2-LP) molecules/liposome. Commercial Lcn2-LIPO is not conjugated with ICAM-1 antibody or IgG. Vehicles were also prepared encapsulating scrambled siRNA (SCR) or Rhodamine-dextran (RD).

ICAM-1 Selective Binding

The TNBC targeting efficiency of immunoliposomes was quantified by flow cytometry. We encapsulated the fluorescent molecule RD (10 kDa) instead of Lcn2 siRNA in ICAM-1 antibody or IgG labeled liposome (ICAM-RD-LP or IgG-RD-LP) formulations. The fluorescent immunoliposomes were used to quantify binding with MDA-MB-231 cells, a representative TNBC cell line.

In **Figure 2**, ICAM-RD-LPs demonstrated 3.54 ± 0.16 fold higher binding than non-specific IgG-RD-LP with MDA-MB-231 cells, which correlates with higher ICAM-1 surface densities on MDA-MB-231 cells (**Figure S3**). Non-neoplastic human mammary epithelial MCF10A cells lack ICAM-1 expression on their cell surface, resulting in negligible ICAM-RD-LP uptake (**Figure 2**). This indicates that ICAM-1-targeted immunoliposomes can selectively target MDA-MB-231 cells over non-neoplastic cells. It is worth noting that ICAM-1 expression in normal organs is substantially less than that of epidermal growth factor receptor (EGFR), a generally accepted TNBC molecular target.(36)

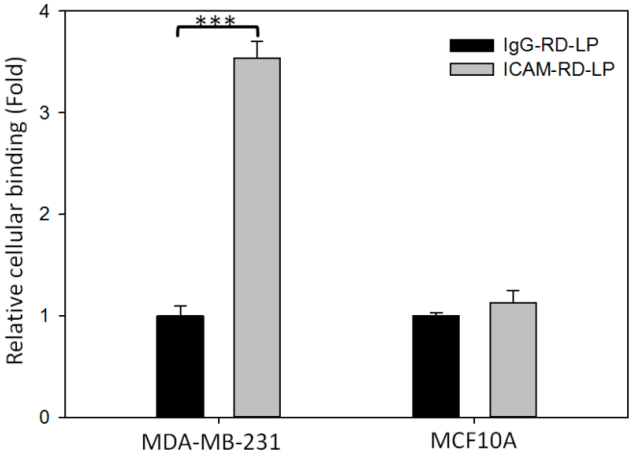

Figure 2. Cellular binding of immunoliposomes in MDA-MB-231 and MCF10A cells. Cells were treated with either ICAM-RD-LP or IgG-RD-LP (control), then characterized via flow cytometry (*** $p<0.001$).

Lipocalin-2 Gene Knockdown

We examined the knockdown efficacy of ICAM-Lcn2-LPs by qRT-PCR. Lcn2 expression was measured after MDA-MB-231 cells were treated with PBS (control), free Lcn2 siRNA, ICAM-SCR-LPs, Lcn2-LIPO, IgG-Lcn2-LPs, and ICAM-Lcn2-LPs. As shown in **Figure 3a,** MDA-MB-231 cells treated with PBS (control), free Lcn2 siRNA and ICAM-SCR-LP demonstrated no change in their Lcn2 expression levels. Lcn2-LIPO and IgG-Lcn2-LP showed a reduction in Lcn2 of 41-56%. ICAM-Lcn2-LP was significantly more efficient than all other formulations, with a reduction in Lcn2 expression of 78.3 ± 1.7% (1.9-fold higher than IgG-Lcn2-LP). This was confirmed by immunoblot assay and densitometric analysis (**Figures 3b and c**). In accordance with Lcn2 gene expression at the transcript levels (**Figure 3a**), ICAM-Lcn2-LP treated MDA-MB-231 cells demostrated a significant Lcn2 protein reduction of 76.1

± 1.7%, which was approximately 1.5-fold higher than either IgG-Lcn2-LP or Lcn2-LIPO treated cells alone. Immunoliposomes targeting EGFR were reported to have 1.36-1.5 fold higher silencing efficiency than the non-specific control; this enhancement was achieved at comparable levels of antibody conjugation.(37) As shown in **Figure 3d,** all formulations at the gene silencing dosage exhibited no cytotoxicity in MDA-MB-231 cells. Combined qRT-PCR and immunoblot results indicated that our engineered TNBC-targeted, siRNA-encapsulating immunoliposomes significantly inhibited the expression of a specific molecular target in TNBC cells at both mRNA and protein levels.

Down-regulation of VEGF

During angiogenesis, tumor cells release VEGF to drive new vessel growth by attracting and activating endothelial cells from the microenvironment.(38) This tumor-induced angiogenesis is critical in the development of a blood supply to support tumor growth and metastasis.(14–16) We have previously discovered that Lcn2 stimulates neovascularization in breast cancer, and that silencing Lcn2 reduces VEGF production.(17,18) Using a specific ELISA for VEGF, we determined the levels of this protein in the conditioned media (CM) harvested from MDA-MB-231 cells treated with six different formulations (**Figure 4**). VEGF was significantly reduced by 58 ± 1 % in CM of ICAM-Lcn2-LP treated MDA-MB-231 cells. In comparison, CM of MDA-MB-231 cells treated with Lcn2-LIPO and IgG-Lcn2-LPs demonstrated a reduction in VEGF by 27 and 19%, respectively. No change in VEGF concentration was observed in the CM of cells treated with either free Lcn2 siRNA or ICAM-SCR-LPs. These findings demonstrated that targeting overexpressed ICAM-1 and silencing Lcn2 simultaneously via ICAM-Lcn2-LP can effectively suppress VEGF secretion from MDA-MB-231 cells.

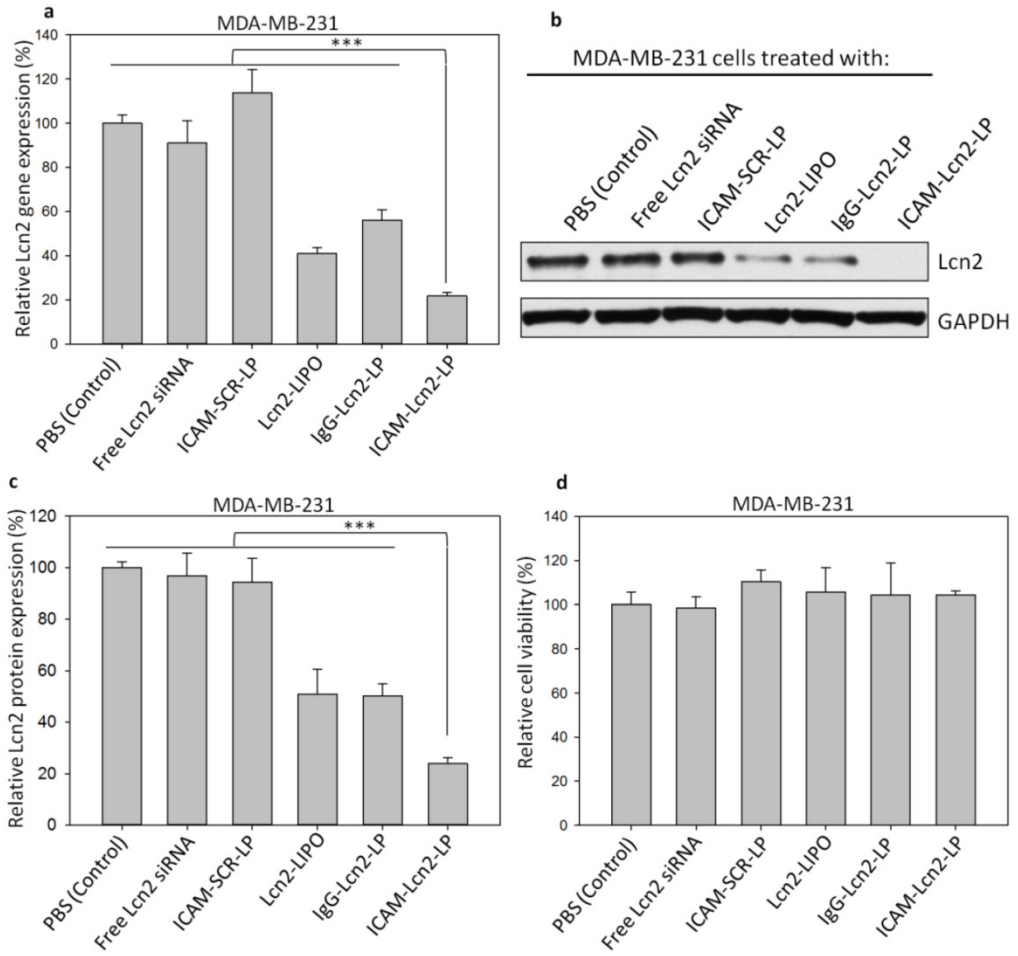

Figure 3. siRNA knockdown of Lcn2 gene expression at the transcript level were determined by qRT-PCR (a). Lcn2 protein levels in MDA-MB-231 cells treated with immunoliposomes were determined by immunoblot assay (b), and quantified by densitometric analysis (c) (*** $p<0.001$). Cytotoxicity of immunoliposomes in MDA-MB-231 cells was determined by Dojindo assay (d).

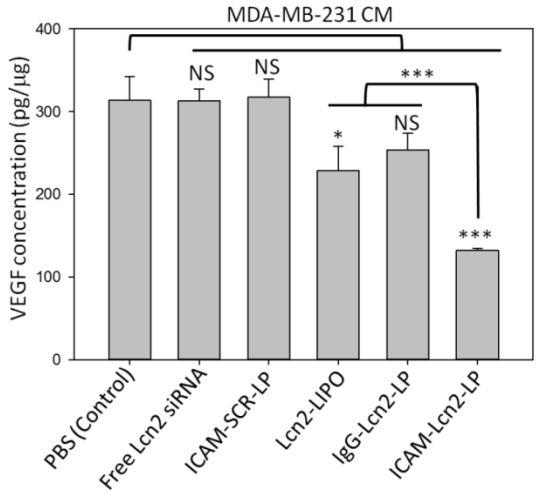

Figure 4. ELISA characterization of VEGF concentration (VEGF/total protein, pg/μg) in the condition media collected from MDA-MB-231 cells treated with immunoliposomes. (NS: no significant difference, * $p<0.05$, *** $p<0.001$).

Angiogenesis Assays

We next determined the anti-angiogenic impact of ICAM-Lcn2-LPs using three in vitro angiogenic assays: human endothelial cell proliferation, migration, and tube formation.(23,24,26) Human microvascular endothelial cells (HMVECs) and human umbilical vein endothelial cells (HUVECs) were chosen as two representative normal human endothelial cell lines. We first examined the effect of ICAM-Lcn2-LP treatment on endothelial cell proliferation. CM harvested from MDA-MB-231 cells treated with the six formulations as described above was added to HMVECs and HUVECs separately to promote cell proliferation for 48 h. As shown in **Figure 5**, there was no impact on proliferation for all the formulations examined. These results also demonstrate the lack of cytotoxicity of these formulations.

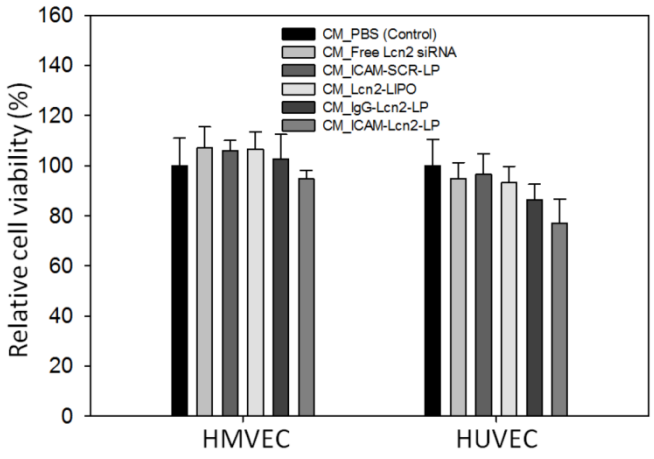

Figure 5. Human endothelial cell proliferation in conditioned media harvested from MDA-MB-231 cells treated with immunoliposomes.

The ability of human endothelial cells to migrate toward TNBC cells was quantified using a transwell migration assay as previously described by us.(18,20,25) In this assay, HMVECs and HUVECs were allowed to migrate through an 8-μm porous membrane using CM harvested from MDA-MB-231 cells treated with the six immunoliposome samples as chemoattractants (**Figures 6a and c**). Cells seeded in the upper chamber were attracted to the VEGF in the CM in the lower chamber. The CM of ICAM-Lcn2-LP-treated cells significantly reduced the number of transmigrated cells by 84% for HMVEC and 53% for HUVEC in comparison with the control CM (**Figures 6 b and d**), which correlates with the VEGF levels in the CM. A comparable inhibitory effect was generated using 2.5 mg/mL of Bevacizumab (humanized anti-VEGF monoclonal antibody), a U.S. Food and Drug Administration (U.S. FDA) -approved angiogenesis inhibitor, however at a dose which is clinically unattainable.(39–41)

Endothelial tube formation is one of the key steps in tumor angiogenesis.(15,42) Given that VEGF is known to stimulate rapid remodeling and capillary tube formation,(38) we hypothesized that ICAM-Lcn2-LP treatment would suppress the VEGF-induced tube formation of human endothelial cells. Indeed, as demonstrated in **Figures 7a and c**, a significant decrease in tube formation was observed in HMVECs and HUVECs in the presence of CM of MDA-MB-231 cells treated with ICAM-Lcn2-LPs. The tube formation activity was further quantified by counting the total number of branches in the tube formation assay. **Figures 7b and d** demonstrated that ICAM-Lcn2-LPs inhibited HMVEC tube formation by 56% and HUVEC by 60%. Lcn2-LIPO and IgG-Lcn2-LP showed much weaker inhibitory effects on tube formation. These results indicate that down-regulation of Lcn2 gene expression by ICAM-Lcn2-LP inhibits TNBC-induced endothelial tube formation. On the basis of these findings, we conclude that the TNBC-targeted delivery of Lcn2 siRNA by ICAM-Lcn2-LP impairs the ability of breast cancer cells to recruit and assemble endothelial cells. Similar inhibition on endothelial cell tube formation was achieved using Bevacizumab at concentrations higher than 100 μg/mL.(39–41)

We next assessed the *in vivo* anti-angiogenic activity of our ICAM-Lcn2-LP using the chick chorioallantoic membrane (CAM) assay, an *in vivo* model of neovascularization.(23,24,27,28) CM harvested from MDA-MB-231 cells treated with different liposomal formulations was applied to the CAM on day 7 and the extent of angiogenesis surrounding the CM-containing substrate was evaluated 48 h later. As shown in **Figure 8**, CM of MDA-MB-231 cells treated

with PBS (sham) increased the density of newly-formed vessels (**Figure 8b arrows**) and this angiogenesis stimulatory effect was significantly inhibited by treatment with ICAM-Lcn2-LP **(Figure 8d)** but not non-specific IgG-Lcn2-LP (**Figure 8c**). Substrate with serum-free media, included as a negative control, exhibited no significant angiogenic effect (**Figure 8a**). The angiogenesis surrounding the substrate was further quantified using a scoring system with the most intense vessel formation scored as 4 and no vessel formation scored as 0.(29) As shown in **Figures 8d and e**, CM of cells treated with ICAM-Lcn2-LP induced significantly less angiogenesis in the CAM assay. These findings demonstrate that treatment with ICAM-Lcn2-LP inhibits the angiogenic activity of TNBC cells *in vivo*.

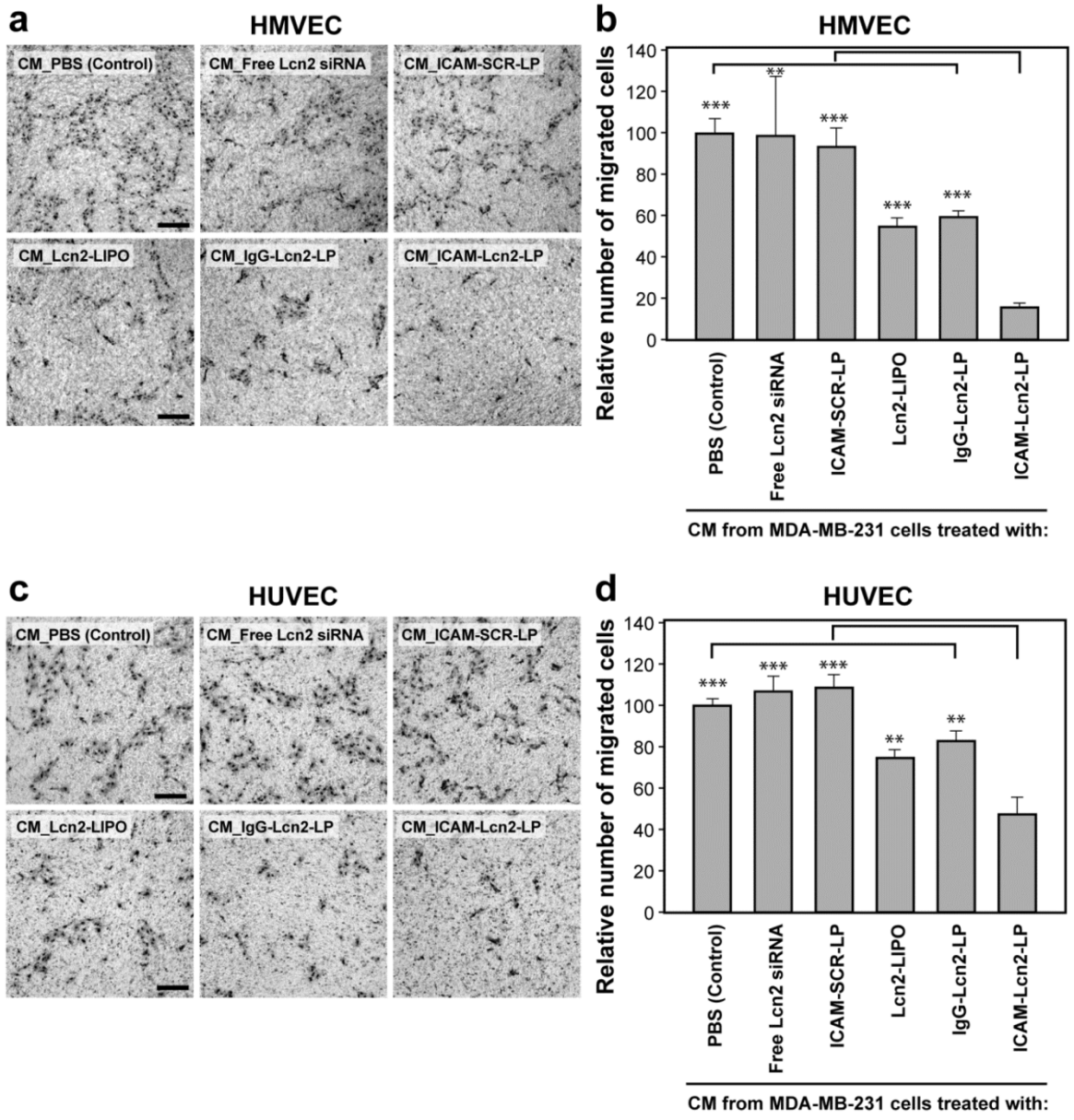

Figure 6. Human endothelial cell (a. HMVEC and c. HUVEC) migration toward conditioned media harvested from MDA-MB-231 cells treated with immunoliposomes. Histogram of quantified migrated cell numbers was shown for HMVEC (b) and HUVEC (d). All scale bars are 100 μm (** p<0.01, *** p<0.001).

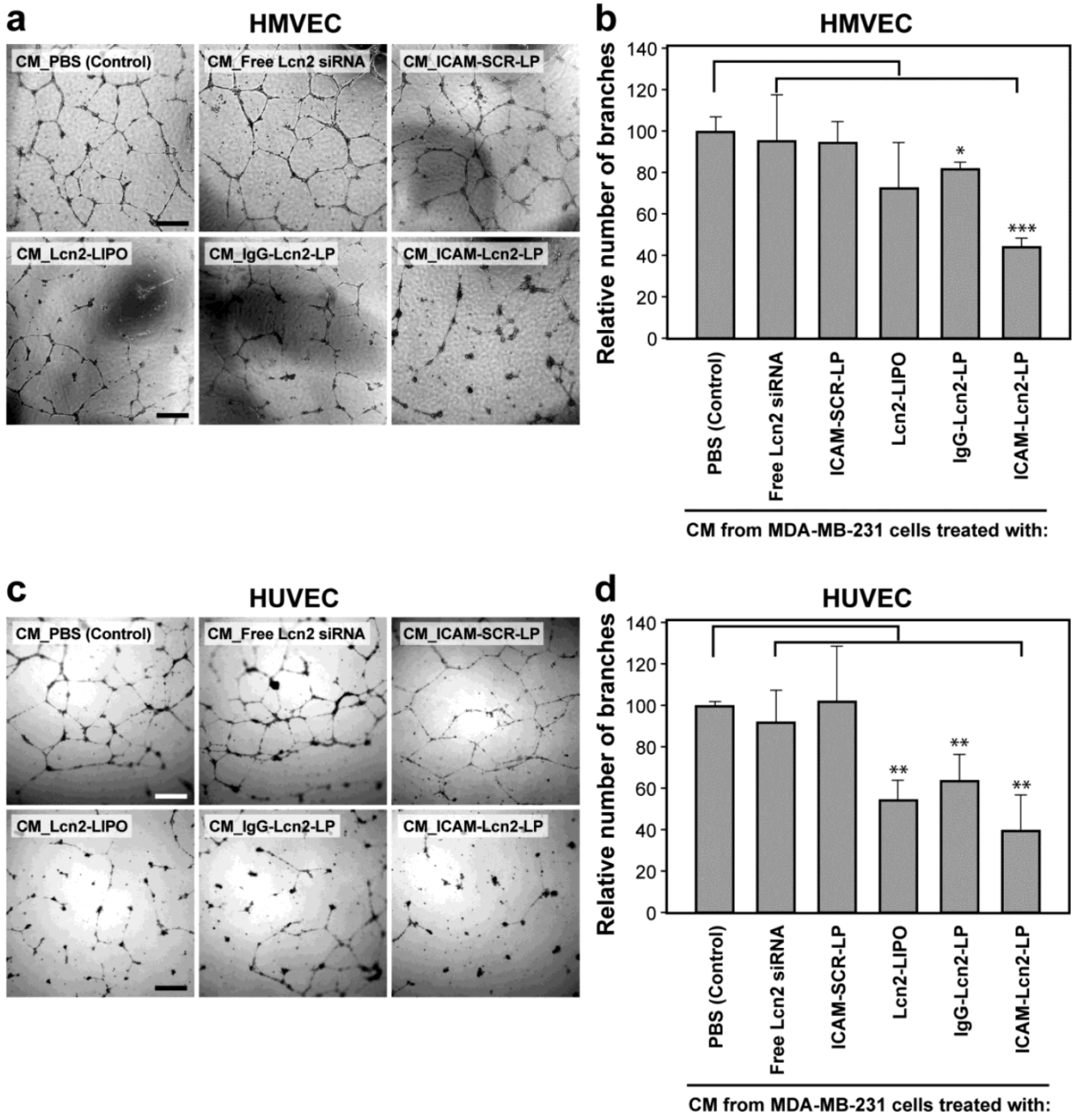

Figure 7. Human endothelial cell (a. HMVEC and c. HUVEC) tube formation in conditioned media harvested from MDA-MB-231 cells treated with immunoliposomes. Number of branches were quantified for (b) HMVEC and (d) HUVEC. All scale bars are 200 μm (* $p<0.05$, ** $p<0.01$, *** $p<0.001$).

Discussion

RNA interference is under intense investigation as a therapeutic approach for breast cancer and other solid tumors.(3,43) We have identified Lcn2 as a therapeutic target that impacts VEGF production, endothelial migration, and *in vivo* angiogenesis.(17,18) Here, we demonstrate that ICAM-1 overexpression on TNBC cells can be exploited to significantly enhance delivery to TNBC cells and increase the transfection efficiency of Lcn2 siRNA, confirming that ICAM-1 is an effective nanomedicine target for TNBC.

We have engineered a TNBC-targeted immunoliposome to meet the urgent clinical need for a TNBC-targeted therapy. This is the first time that ICAM-1, a recently identified TNBC-molecular target, has been used as a TNBC-specific liposomal therapy for siRNA delivery. HER2 antibody-conjugated immunoliposomes demonstrated clinical effectiveness and acceptable human safety profiles in Phase I clinical trials for the treatment of HER2+ breast cancer.(44–46) PEG (2 kDa) was functionalized on our TNBC-targeted immunoliposome surface by doping DSPE-PEG-COOH into the lipid bilayer at a molar ratio of 5%. This PEGylation step provides our TNBC-targeted immunoliposome with a "stealth"

function and can significantly prolong the circulation time.(32,33) PEGylation is a strategy utilized in the liposomal therapeutic, Doxil, to increase circulation time.(47) Lastly, the pH-sensitive lipid, DODAP, has been incorporated into the lipid bilayer of our TNBC-targeted immunoliposome to facilitate siRNA escape from endosomes and enhance siRNA transfection efficiency (as seen in **Figures S5 and S6**).(30,31) Taken together, our TNBC-targeted immunoliposome demonstrates a number of advantages, and is significantly more effective, than the commercial siRNA transfection reagent, Lipofectamine (as demonstrated in **Figure 3a**). Our TNBC-targeted immunoliposome can achieve an efficient siRNA silencing effect (about 80% siRNA knockdown) at a siRNA dosage of 100 nM, which is significantly lower than many other existing siRNA nanocarrier formulations in the literature, for example: 200 nM siRNA for cationic lipid-assisted polyethylene glycol–polylactic acid (PEG-PLA) nanoparticles,(48) 250 nM siRNA for anti-EGFR antibody conjugated immunoliposomes,(37) and over 1000 nM siRNA for PLA layer by layer nanoparticles.(49)

Several groups have reported the use of nanoscale drug delivery systems (DDS) for anti-angiogenic therapies.(50–52) Kim et al. reported that RGD peptide encapsulated glycol chitosan nanoparticles significantly lowered HUVEC cell adhesion.(50) Another study using a VEGF siRNA-lipofectamine complex showed a significant reduction of endothelium tube formation.(51) However, anti-angiogenic approaches that lack tumor specificity have had limited success in clinical trials.(53,54) Towards this end, we have engineered a novel strategy that targets tumors via ICAM-1 and triggers delivery to the cytoplasm via a pH-sensitive lipid.

The purpose of the present study was to develop a novel liposomal system to specifically deliver Lcn2 siRNA to TNBCs and to inhibit angiogenesis. Targeted therapies against TNBC remain a long-standing challenge due to the lack of molecular targets. The ICAM-Lcn2-LPs described here address this need. In this study, we verified that ICAM-1 antibody-conjugated, siRNA-encapsulating immunoliposomes were capable of targeting TNBC cells and silencing the Lcn2 gene. The collective *in vitro* results reported here demonstrated that ICAM-Lcn2-LPs inhibited downstream VEGF secretion from TNBC cells. The anti-angiogenic properties of ICAM-Lcn2-LP – as shown by reductions in TNBC-induced endothelial cell tube formation and migration - were observed using two types of human endothelial cells (HMVEC and HUVEC). Further, our findings from an *in vivo* CAM assay confirmed that our TNBC-targeting strategy significantly blocked TNBC-induced blood vessel recruitment from the surrounding microenvironment. This drug delivery system may be a successful model for the design of anti-angiogenic therapies.

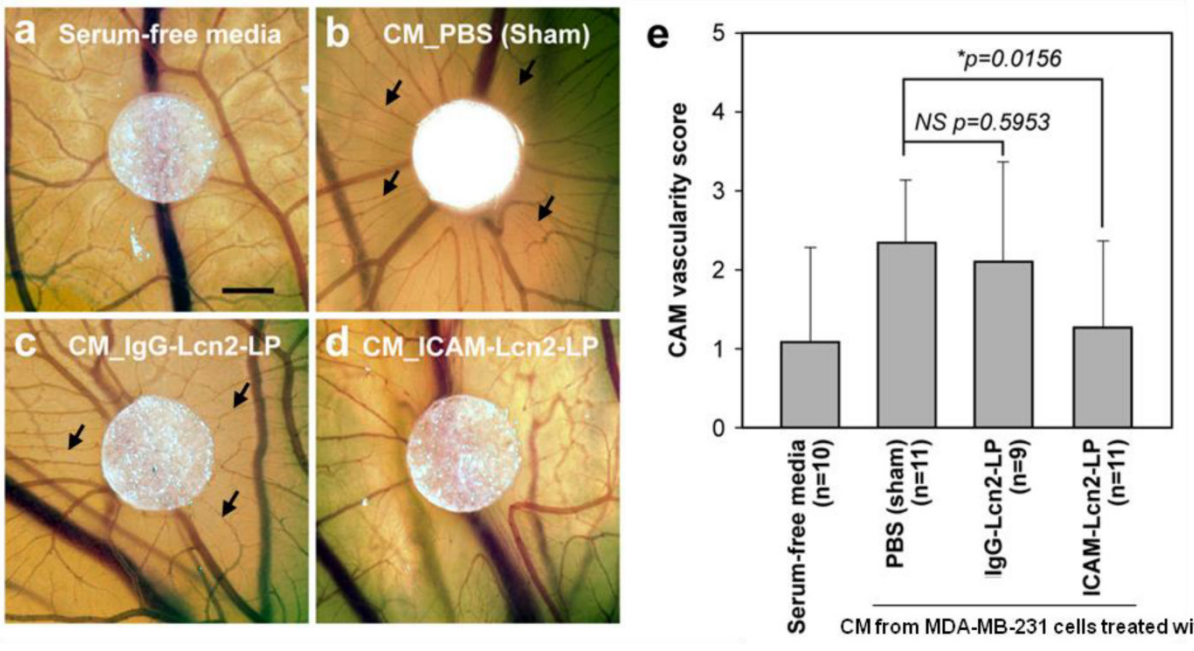

Figure 8. Conditioned media from MDA-MB-231 cells treated with ICAM-Lcn2-LP inhibits *in vivo* angiogenesis in the CAM assay. Representative micrographs are shown for CAMs treated with serum-free media (a), or CM from MDA-MB-231 cells treated with PBS (sham) (b), CM from MDA-MB-231 cells treated with IgG-Lcn2-LP (c), and CM from MDA-MB-231 cells treated with ICAM-Lcn2-LP (d). Scale bar is 1 mm, and arrows point to areas of newly formed blood vessels. CAM vascularity for each experimental group was scored on a scale of 0–4 (e). (NS: no significant difference,* $p<0.05$).

The current report represents a proof of concept study of a novel TNBC-targeted, Lcn2-silencing therapy. Liposomal nanocarriers are a versatile platform to deliver imaging agents (e.g. iron oxide nanoparticles,(55) copper-radionuclide (64Cu)(56)) as well as therapeutic molecules (e.g. doxorubicin,(47) siRNAs(5,6)). Furthermore, stimuli-responsive liposomes have been developed to improve the intracellular delivery of nucleic acids.(57,58) Herein, we created and evaluated a novel TNBC-targeted, siRNA encapsulating immunoliposome that can reduce Lcn2 levels and hinder tumor angiogenesis.

Conclusion

In summary, we have successfully engineered a novel immunoliposome that synergistically couples TNBC-targeting with Lcn2 siRNA silencing. Synthesized ICAM-1-targeted Lcn2 siRNA encapsulating liposomes significantly suppress *in vitro* and *in vivo* angiogenic activities of TNBC cells. The modular design introduced in this study provides a new platform for future TNBC-targeted therapeutics.

Supplementary Material

Figures S1- S6.
http://www.thno.org/v06p0001s1.pdf

Acknowledgements

D. Auguste acknowledges the support of the National Institutes of Health (NIH), National Cancer Institute Grant 1DP2CA174495. M. Moses acknowledges the support of NIH R01CA185530 and the support of the Breast Cancer Research Foundation.

Competing Interests

The authors have declared that no competing interest exists.

References

1. Kim DH, Rossi JJ. Strategies for silencing human disease using RNA interference. Nat Rev Genet. 2007;8:173–84.
2. Devi GR. siRNA-based approaches in cancer therapy. Cancer Gene Ther. 2006;13:819–29.
3. Oh Y-K, Park TG. siRNA delivery systems for cancer treatment. Adv Drug Deliv Rev. 2009;61:850–62.
4. Morrissey DV, Lockridge JA, Shaw L, Blanchard K, Jensen K, Breen W, et al. Potent and persistent in vivo anti-HBV activity of chemically modified siRNAs. Nat Biotechnol. 2005;23:1002–7.
5. Liu X, Madhankumar AB, Slagle-Webb B, Sheehan JM, Surguladze N, Connor JR. Heavy chain ferritin siRNA delivered by cationic liposomes increases sensitivity of cancer cells to chemotherapeutic agents. Cancer Res. 2011;71:2240–9.
6. Yonenaga N, Kenjo E, Asai T, Tsuruta A, Shimizu K, Dewa T, et al. RGD-based active targeting of novel polycation liposomes bearing siRNA for cancer treatment. J Controlled Release. 2012;160:177–81.
7. Meng H, Mai WX, Zhang H, Xue M, Xia T, Lin S, et al. Codelivery of an optimal drug/siRNA combination using mesoporous silica nanoparticles to overcome drug resistance in breast cancer *in vitro* and *in vivo*. ACS Nano. 2013;7:994–1005.
8. Dahlman JE, Barnes C, Khan OF, Thiriot A, Jhunjunwala S, Shaw TE, et al. In vivo endothelial siRNA delivery using polymeric nanoparticles with low molecular weight. Nat Nanotechnol. 2014;9:648–55.
9. Foulkes WD, Smith IE, Reis-Filho JS. Triple-Negative Breast Cancer. N Engl J Med. 2010;363:1938–48.
10. Ovcaricek T, Frkovic S, Matos E, Mozina B, Borstnar S. Triple negative breast cancer - prognostic factors and survival. Radiol Oncol. 2011;45.
11. Slamon D, Eiermann W, Robert N, Pienkowski T, Martin M, Press M, et al. Adjuvant trastuzumab in HER2-positive breast cancer. N Engl J Med. 2011;365:1273–83.
12. Yu K-D, Wu J, Shen Z-Z, Shao Z-M. Hazard of breast cancer-specific mortality among women with estrogen receptor-positive breast cancer after five years from diagnosis: implication for extended endocrine therapy. J Clin Endocrinol Metab. 2012;97:E2201–9.
13. Guo P, Huang J, Wang L, Jia D, Yang J, Dillon DA, et al. ICAM-1 as a molecular target for triple negative breast cancer. Proc Natl Acad Sci. 2014;111:14710–5.
14. Folkman J. Tumor angiogenesis: therapeutic implications. N Engl J Med. 1971;285:1182–6.
15. Harper J, Moses MA. Molecular regulation of tumor angiogenesis: mechanisms and therapeutic implications. EXS. 2006;223–68.
16. Roy R, Zhang B, Moses MA. Making the cut: protease-mediated regulation of angiogenesis. Exp Cell Res. 2006;312:608–22.
17. Fernández CA, Yan L, Louis G, Yang J, Kutok JL, Moses MA. The matrix metalloproteinase-9/neutrophil gelatinase-associated lipocalin complex plays a role in breast tumor growth and is present in the urine of breast cancer patients. Clin Cancer Res 2005;11:5390–5.
18. Yang J, McNeish B, Butterfield C, Moses MA. Lipocalin 2 is a novel regulator of angiogenesis in human breast cancer. FASEB J. 2013;27:45–50.
19. Yang J, Moses MA. Lipocalin 2: a multifaceted modulator of human cancer. Cell Cycle Georget Tex. 2009;8:2347–52.
20. Yang J, Bielenberg DR, Rodig SJ, Doiron R, Clifton MC, Kung AL, et al. Lipocalin 2 promotes breast cancer progression. Proc Natl Acad Sci. 2009;106:3913–8.
21. Guo P, You J-O, Yang J, Jia D, Moses MA, Auguste DT. Inhibiting metastatic breast cancer cell migration via the synergy of targeted, pH-triggered siRNA delivery and chemokine axis blockade. Mol Pharm. 2014;11:755–65.
22. Guo P, You J-O, Yang J, Moses MA, Auguste DT. Using breast cancer cell CXCR4 surface expression to predict liposome binding and cytotoxicity. Biomaterials. 2012;33:8104–10.
23. Fernandez CA. Structural and Functional Uncoupling of the enzymatic and angiogenic inhibitory activities of tissue inhibitor of metalloproteinase-2 (TIMP-2): Loop is a novel angiogenesis inhibitor. J Biol Chem. 2003;278:40989–95.
24. Foradori MJ, Chen Q, Fernandez CA, Harper J, Li X, Tsang PCW, et al. Matrilin-1 is an inhibitor of neovascularization. J Biol Chem. 2014;289:14301–9.
25. Roy R, Rodig S, Bielenberg D, Zurakowski D, Moses MA. ADAM12 transmembrane and secreted isoforms promote breast tumor growth: a distinct role for ADAM12-S protein in tumor metastasis. J Biol Chem. 2011;286:20758–68.
26. Akino T, Han X, Nakayama H, McNeish B, Zurakowski D, Mammoto A, et al. Netrin-1 promotes medulloblastoma cell invasiveness and angiogenesis, and demonstrates elevated expression in tumor tissue and urine of patients with pediatric medulloblastoma. Cancer Res. 2014;74:3716–26.
27. Moses MA, Sudhalter J, Langer R. Identification of an inhibitor of neovascularization from cartilage. Science. 1990;248:1408–10.
28. Moses MA, Wiederschain D, Wu I, Fernandez CA, Ghazizadeh V, Lane WS, et al. Troponin I is present in human cartilage and inhibits angiogenesis. Proc Natl Acad Sci. 1999;96:2645–50.
29. Ponce ML, Kleinmann HK. The Chick Chorioallantoic Membrane as an In Vivo Angiogenesis Model. In: Bonifacino JS, Dasso M, Harford JB, Lippincott-Schwartz J, Yamada KM, editors. Curr Protoc Cell Biol. Hoboken, NJ, USA: John Wiley & Sons, Inc.; 2003
30. You J-O, Almeda D, Ye GJ, Auguste DT. Bioresponsive matrices in drug delivery. J Biol Eng. 2010;4:15.
31. Hillaireau H, Couvreur P. Nanocarriers' entry into the cell: relevance to drug delivery. Cell Mol Life Sci. 2009;66:2873–96.
32. Photos PJ, Bacakova L, Discher B, Bates FS, Discher DE. Polymer vesicles in vivo: correlations with PEG molecular weight. J Control Release Off J Control Release Soc. 2003;90:323–34.
33. Harris JM, Chess RB. Effect of pegylation on pharmaceuticals. Nat Rev Drug Discov. 2003;2:214–21.
34. Liu D, Mori A, Huang L. Role of liposome size and RES blockade in controlling biodistribution and tumor uptake of GM1-containing liposomes. Biochim Biophys Acta. 1992;1104:95–101.
35. Nagayasu null, Uchiyama null, Kiwada null. The size of liposomes: a factor which affects their targeting efficiency to tumors and therapeutic activity of liposomal antitumor drugs. Adv Drug Deliv Rev. 1999;40:75–87.
36. Uhlen M, Oksvold P, Fagerberg L, Lundberg E, Jonasson K, Forsberg M, et al. Towards a knowledge-based Human Protein Atlas. Nat Biotechnol. 2010;28:1248–50.
37. Gao J, Liu W, Xia Y, Li W, Sun J, Chen H, et al. The promotion of siRNA delivery to breast cancer overexpressing epidermal growth factor receptor through anti-EGFR antibody conjugation by immunoliposomes. Biomaterials. 2011;32:3459–70.
38. Leung D, Cachianes G, Kuang W, Goeddel D, Ferrara N. Vascular endothelial growth factor is a secreted angiogenic mitogen. Science. 1989;246:1306–9.
39. Carneiro A, Falcão M, Azevedo I, Falcão Reis F, Soares R. Multiple effects of bevacizumab in angiogenesis: implications for its use in age-related macular degeneration. Acta Ophthalmol (Copenh). 2009;87:517–23.

40. Sharma RK, Balaiya S, Chalam KV. Bevacizumab suppression of establishment of micrometastases in experimental ocular melanoma. Invest Ophthalmol Vis Sci. 2010;51:6906–6906.
41. Han YS, Lee JE, Jung JW, Lee JS. Inhibitory effects of bevacizumab on angiogenesis and corneal neovascularization. Graefes Arch Clin Exp Ophthalmol. 2009;247:541–8.
42. Moses MA, Harper J, Fernández CA. A role for antiangiogenic therapy in breast cancer. Curr Oncol Rep. 2004;6:42–8.
43. Schiffelers RM. Cancer siRNA therapy by tumor selective delivery with ligand-targeted sterically stabilized nanoparticle. Nucleic Acids Res. 2004;32:e149–e149.
44. Wickham T, Futch K. Abstract P5-18-09: A Phase I Study of MM-302, a HER2-targeted Liposomal Doxorubicin, in Patients with Advanced, HER2-Positive Breast Cancer. Cancer Res. 2012;72:P5–18 – 09.
45. Geretti E, Reynolds J, Hendriks B, Eckelhofer I, Espelin C, Gaddy D, et al. Abstract C90: HER2-targeted liposomal doxorubicin MM-302 has a favorable cardiosafety profile in preclinical models. Mol Cancer Ther. 2011;10:C90–C90.
46. Hendriks B, Shields A, Siegel BA, Miller K, Munster P, Ma C, et al. 55P * PET/CT imaging of 64Cu-labelled HER2 liposomal doxorubicin (64Cu-MM-302) quantifies variability of liposomal drug delivery to diverse tumor lesions in HER2-positive breast cancer patients. Ann Oncol. 2014;25:i19–i19.
47. O'Brien MER. Reduced cardiotoxicity and comparable efficacy in a phase III trial of pegylated liposomal doxorubicin HCl (CAELYXTM/Doxil") versus conventional doxorubicin for first-line treatment of metastatic breast cancer. Ann Oncol. 2004;15:440–9.
48. Liu Y, Zhu Y-H, Mao C-Q, Dou S, Shen S, Tan Z-B, et al. Triple negative breast cancer therapy with CDK1 siRNA delivered by cationic lipid assisted PEG-PLA nanoparticles. J Controlled Release. 2014;192:114–21.
49. Deng ZJ, Morton SW, Ben-Akiva E, Dreaden EC, Shopsowitz KE, Hammond PT. Layer-by-layer nanoparticles for systemic codelivery of an anticancer drug and siRNA for potential triple-negative breast cancer treatment. ACS Nano. 2013;7:9571–84.
50. Kim J-H, Kim Y-S, Park K, Kang E, Lee S, Nam HY, et al. Self-assembled glycol chitosan nanoparticles for the sustained and prolonged delivery of antiangiogenic small peptide drugs in cancer therapy. Biomaterials. 2008;29:1920–30.
51. Raskopf E, Vogt A, Sauerbruch T, Schmitz V. siRNA targeting VEGF inhibits hepatocellular carcinoma growth and tumor angiogenesis in vivo. J Hepatol. 2008;49:977–84.
52. Di Paolo D, Pastorino F, Zuccari G, Caffa I, Loi M, Marimpietri D, et al. Enhanced anti-tumor and anti-angiogenic efficacy of a novel liposomal fenretinide on human neuroblastoma. J Controlled Release. 2013;170:445–51.
53. Kümler I, Christiansen OG, Nielsen DL. A systematic review of bevacizumab efficacy in breast cancer. Cancer Treat Rev. 2014;40:960–73.
54. Mackey JR, Kerbel RS, Gelmon KA, McLeod DM, Chia SK, Rayson D, et al. Controlling angiogenesis in breast cancer: a systematic review of anti-angiogenic trials. Cancer Treat Rev. 2012;38:673–88.
55. Mikhaylov G, Mikac U, Magaeva AA, Itin VI, Naiden EP, Psakhye I, et al. Ferri-liposomes as an MRI-visible drug-delivery system for targeting tumours and their microenvironment. Nat Nanotechnol. 2011;6:594–602.
56. Petersen AL, Binderup T, Rasmussen P, Henriksen JR, Elema DR, Kjær A, et al. 64Cu loaded liposomes as positron emission tomography imaging agents. Biomaterials. 2011;32:2334–41.
57. Mura S, Nicolas J, Couvreur P. Stimuli-responsive nanocarriers for drug delivery. Nat Mater. 2013;12:991–1003.
58. Ganta S, Devalapally H, Shahiwala A, Amiji M. A review of stimuli-responsive nanocarriers for drug and gene delivery. J Controlled Release. 2008;126:187–204.